18. D. Stöffler, *Fortschr. Mineral.* **49**, 50 (1972).
19. _____, *Fortschr. Mineral.* **51**, 256 (1974).
20. A. El Goresy *et al.*, *Am. Mineral.* **86,** 611 (2001).
21. The x-ray facility used in this study includes a rotating anode generator (18 kW), a capillary collimating system, and a charge-coupled device (CCD) area detector. The radiation from the rotating anode with a molybdenum target is filtered by a zirconium foil so that the intensity of Kβ x-ray reflection is 1% of that of Kα x-ray reflection. The beam of initial size 1 mm by 0.5 mm is collimated to 0.1-mm diameter using the capillary system. A special collimator was used to reduce the size of the x-ray spot to 40 μm full width at half maximum. The diffracted x-rays were collected on a detector with an area of 512 by 512 pixels. Data were acquired at fixed 2θ settings of 15, 25, and 30 and a sample-to-detector distance of 210 mm. Collection time in different points varied from 15 min to 12 hours. Settings of the detector were calibrated with external independent standards (W, MgO, and Al_2O_3) at each position of the detector. The sample disc was mounted on a 0.8-mm hole in a large steel disc that was loaded onto the goniometer stage. We rotated the sample plate 30° from the initial position normal to the x-ray beam with a step of 1° in the ω axis during data collection. The position of the collimated x-ray beam penetrating through the rutile-ZrO_2–structured polymorph-bearing assemblage was continuously monitored on a screen with a CCD camera.
22. V. Stähle, P. Gillet, M. Chen, A. El Goresy, *Meteorit. Planet. Sci.* (1999).
23. _____, unpublished data.
24. E. C. T. Chao, *Science* **156**, 192 (1967).
25. P. S. DeCarli, A. P. Jones, G. D. Price, *Laboratory Impact Experiments and Calculations vs. Natural Impact Events. Catastrophic Events & Mass Extinctions: Impacts and Beyond* (Lunar and Planetary Institute, Vienna, 2000).
26. P. S. DeCarli, E. Bowden, T. G. Sharp, A. P. Jones, G. D. Price, *Lunar Planet Sci.* **XXXII**, abstract 3090 (2001).
27. A. El Goresy, L. S. Dubrovinsky, T. G. Sharp, S. K. Saxena, M. Chen, *Science* **288**, 1632 (2000).
28. M. Okuno, B. Reynard, Y. Shimada, Y. Syono, C. Williame, *Phys. Chem. Mineral.* **26**, 304 (1999).
29. V. L. Masaitis, *Meteorit. Planet. Sci.* **33**, 349 (1998).
30. M.C. was supported by the National Science Foundation of China (grant 49825132) and Deutsche Forschungsgemeinschaft (Go 315/15-1). The manuscript benefited from constructive reviews by two anonymous reviewers. We are indebted to O. Medenbach of Ruhr Universität Bochum for his aid in precisely coring out the assemblage depicted in Fig. 1 for microbeam x-ray diffraction.

8 May 2001; accepted 11 July 2001

Large Groundwater Strontium Flux to the Oceans from the Bengal Basin and the Marine Strontium Isotope Record

Asish R. Basu,[1]* Stein B. Jacobsen,[2] Robert J. Poreda,[1] Carolyn B. Dowling,[1] Pradeep K. Aggarwal[3]

Strontium concentration and isotopic data for subsurface flowing groundwaters of the Ganges-Brahmaputra (G-B) delta in the Bengal Basin demonstrate that this is a potentially significant source of strontium to the oceans, equal in magnitude to the dissolved strontium concentration carried to the oceans by the G-B river waters. The strontium concentrations of groundwaters are higher by a factor of about 10 than typical G-B river waters and they have similar $^{87}Sr/^{86}Sr$ ratio to the river waters. These new data suggest that the present contribution of the G-B system to the rise in $^{87}Sr/^{86}Sr$ ratio in seawater is higher by at least a factor of 2 to 5 than the average over the past 40 million years.

Variations of $^{87}Sr/^{86}Sr$ ratio in seawater are primarily due to variations in continental erosion rates as well as variations in the Sr isotopic composition of this input to the oceans (*1, 2*). Thus, changes in this isotopic ratio are frequently linked to major tectonic events (*3, 4*) and have been used to constrain the problem of Snowball Earth glaciations (*5*). The $^{87}Sr/^{86}Sr$ ratio of seawater has increased from about 0.7078 to 0.7092 over the past 40 million years (My). This rapid increase has been attributed to the Himalayan uplift, following the India-Asia continental collision (*2*), which is believed to have contributed Sr with particularly high $^{87}Sr/^{86}Sr$ ratios to the oceans through the major rivers draining the Himalayas (*3, 4, 6, 7*). The Himalayan uplift has also been suggested as the major cause of the global climate cooling for the past 40 My, because of the increase in chemical weathering of silicates and the resulting decrease of atmospheric CO_2 concentration (*8*).

Most workers accept the importance of the contribution of Himalayan river water dissolved Sr for the marine budget, although the sources and the amount of this Sr flux remain problematic (*9*). Various calculations based on Sr isotopic compositions and Sr concentrations of the G-B rivers indicate that the Himalayan discharge accounts for a large fraction of the observed increase in the marine $^{87}Sr/^{86}Sr$ ratio over the past 40 My (*4, 6*). However, a study of Himalayan riverine $^{187}Os/^{188}Os$ (*10*) could not explain the observed correlated Sr-Os isotopic shift in the marine record by Himalayan input. There is also uncertainty whether the Sr flux and its isotopic composition are primarily controlled by the weathering of silicate minerals (*6, 9, 11, 12*) or are controlled by weathering of metacarbonates that reequilibrated with silicates with high $^{87}Sr/^{86}Sr$ during metamorphism (*7, 13, 14*), or both.

Most earlier studies focused on the weathering of high Himalayan rocks. Here, we are concerned with the effect of groundwater-sediment interaction processes in the G-B flood plain of the Bengal Basin (Fig. 1) in controlling the budget of oceanic Sr as well as the Sr isotopic composition of seawater. This study was prompted by the recent discovery of large groundwater flux on a regional scale to coastal waters (*15*) and that desorption of ^{226}Ra and Ba from deltaic sediments in this area is a significant source of these elements in the waters of the Bay of Bengal (*16*). There is clear evidence of a large groundwater discharge with high Ra and Ba fluxes to the ocean from the G-B rivers during low river discharge (*17*).

For this study, we collected 61 groundwater samples from the southern part of Bangladesh between the Ganges (Padma), Brahmaputra, and Meghna rivers and their tributaries, and nine groundwater samples just north and south of Calcutta in the western part of the basin (Fig. 1). The water samples come from depths of 10 to 350 m. We also collected river waters from six sites of the G-B system within and adjacent to the Bengal Basin (Fig. 1 and Table 1). All the river and groundwater samples were collected during the dry season in January through May and were filtered (0.2 μm pore size) and acidified on site. The Sr concentration and $^{87}Sr/^{86}Sr$ ratios are reported in Table 1. For individual sites where more than one groundwater sample was analyzed from different depths, Table 1 gives the range and average values for Sr. For many of the groundwater samples, we also examined other chemical characteristics, such as dissolved cations and anions, carbon, oxygen, and hydrogen isotopes for all samples, and ^{3}H-^{3}He ages for several of the samples. Here, we are concerned mostly with the $^{87}Sr/^{86}Sr$ and Sr concentrations in these waters, and implications of a groundwater Sr flux on the marine Sr budget.

The Sr concentrations in the groundwater

[1]Department of Earth and Environmental Sciences, University of Rochester, Rochester, NY 14627, USA. [2]Department of Earth and Planetary Sciences, Harvard University, Cambridge, MA 01238, USA. [3]Isotope Hydrology Section, International Atomic Energy Agency, Post Office Box 100, A1400, Vienna, Austria.

*To whom correspondence should be addressed. E-mail: abasu@earth.rochester.edu

show a variable range, with a significant number of samples falling in the range of 4 to 6 μmol/liter. Some samples, which are not included in Table 1, show much higher concentrations (14 to 53 μmol/liter) and are from localities near the coastal regions. As shown by their high Cl content, these very high Sr concentrations are due to mixing with seawater. However, all the other groundwaters listed in Table 1 have been shown to be free of a seawater component, because of their low and uniform Cl contents. In contrast with the groundwaters, the Bengal Basin river waters show much lower concentrations of Sr (~0.5 μmol/liter), similar to or higher than typical Sr contents of the G-B rivers and their tributaries outside the Bengal Basin (*9, 18*). From the average Sr flux of Galy *et al.* (*9*) and the average water flux used by Galy and France-Lanord (*19*), we obtain an average Sr concentration for the G-B river system of 0.61 μmol/liter. Because these rivers discharge into the oceans through the Bengal Basin delta, the flood plain waters should be of utmost significance in estimating the isotopic composition of the Sr flux to the ocean. The strong seasonal variability and low Sr contents of the river water during the monsoon (*9*) should also be considered. Overall, we estimate from our measurements of the Bengal flood plains (Table 1) that the groundwater Sr concentrations are about 10 times higher than that of the river waters.

Next, we compared the $^{87}Sr/^{86}Sr$ compositions of the Bengal Basin groundwater with those of the adjacent surface water flow in the rivers (Fig. 2). The $^{87}Sr/^{86}Sr$ ratios in waters of the Bengal Basin rivers are within the same range as those of the groundwater (Table 1 and Fig. 2). Seasonal variability in the G-B rivers has recently been noted (*9*); in particular these rivers appear to show low Sr concentrations and higher $^{87}Sr/^{86}Sr$ ratios during the monsoon (*9*) as shown in Fig. 2. In general, higher $^{87}Sr/^{86}Sr$ ratios and lower concentrations of Sr are the characteristic features of the Himalayan drainage outside the Bengal Basin (*3, 6, 7, 9, 11–14*). The Bengal Basin flood plain, where the surface discharge has similar $^{87}Sr/^{86}Sr$ signatures as those of the groundwaters, deserves further scrutiny because the rivers may show generally higher or similar Sr concentrations compared to those outside the basin, as reported by previous workers and summarized in Galy *et al.* (*9*). Note also that in Table 1, coastal groundwaters and river waters, as well as the Brahmaputra, have similar $^{87}Sr/^{86}Sr$ (typically ~0.717 to 0.720), and inland groundwaters are similar to the Ganges and its tributary (typically ~0.720 to 0.730) as measured in two sites near Farakka and Calcutta inside the basin (Fig. 1). The very high $^{87}Sr/^{86}Sr$ ratios in Himalayan headwaters of the Ganges are not seen in the Bengal Basin. Most of the variability in groundwater $^{87}Sr/^{86}Sr$ ratio is seen at shallow depths of up to 60 m; below this depth, there is a tendency for the water to have a narrow range in $^{87}Sr/^{86}Sr$ composition between 0.715 to 0.725.

For the present study, an estimate of groundwater annual recharge rate can be made from our ^{3}H-^{3}He isotopic ages (*20, 21*). An average recharge estimate of 0.6 ± 0.2 m/year (*21*) over the entire G-B flood plain (300,000 km^2) translates into a steady-state groundwater flux to the Bay of Bengal of 0.2×10^{15} liter/year, equal to ~19% of the surface water flux (1.07×10^{15} liter/year) to the Bay of Bengal. Independent confirmation of the magnitude of this groundwater discharge comes from the agreement between the Ba flux obtained by multiplying our observed groundwater Ba av-

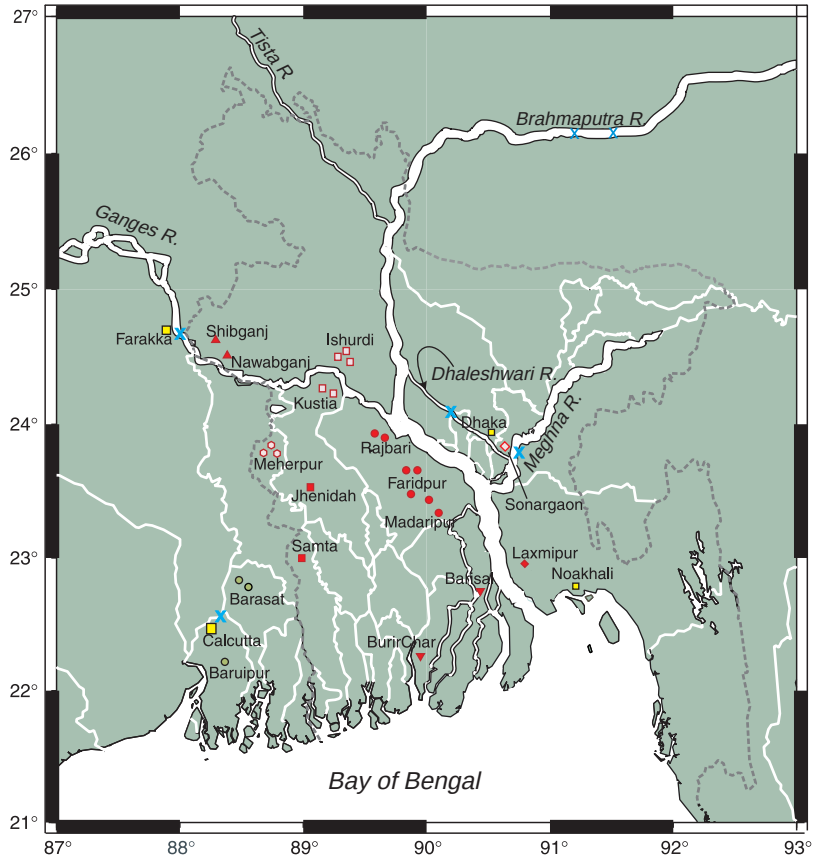

Fig. 1. Map of the Bengal Basin showing the main courses of the Ganges-Brahmaputra and their tributaries and the sample locations for this study. River water locations are shown by crosses, and the groundwater sites are shown by filled symbols. Townships are in open squares.

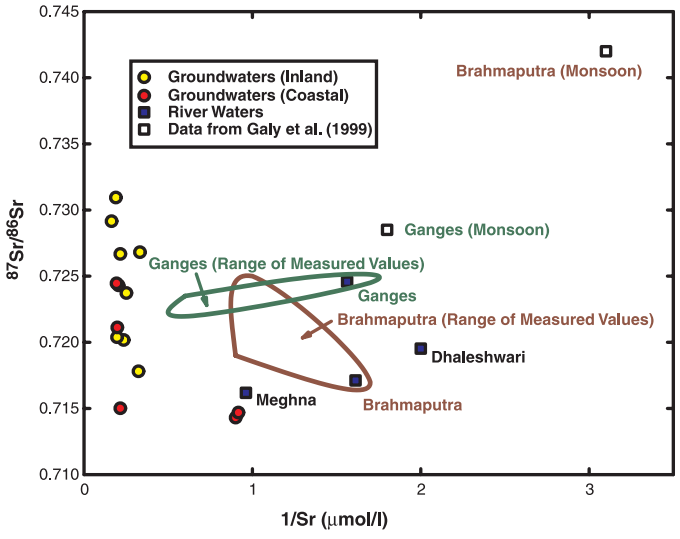

Fig. 2. Strontium concentrations and $^{87}Sr/^{86}Sr$ of groundwaters and river waters of the Bengal Basin. These waters are used to characterize the present-day discharge of Sr to the oceans via the G-B flood plain. Groundwaters and river waters are averages from Table 1, except for the monsoon values (open squares) of Galy *et al.* (*9*). The fields showing the range of measured values include both our new data as well as the data summarized by Galy *et al.* (*9*), except for the river water measurements in the monsoon season.

erage of 1.2 μmol/liter with the groundwater (G-B) flux (= 2.4×10^8 mol/year) and the Ba discharge given by Moore (*17*) based on the correlated Ba-Ra excesses in the Bay of Bengal (3×10^8 to 30×10^8 mol/year). The fact that our groundwater estimate falls at the low end of the estimate by Moore indicates that we are not severely overestimating the magnitude of this discharge.

The first part of Table 2 gives the Sr isotope balance for the G-B rivers. From our new data in Table 1, in addition to the Galy *et al.* data, it is clear that the average Sr isotopic composition of the G-B rivers must be between the high value of 0.7295 favored by Galy *et al.* (*9*) and our much lower value for the Brahmaputra (0.717). The higher $^{87}Sr/^{86}Sr$ value of Galy *et al.* (*9*) reflects, in part, their use of data from the monsoon season when the values can be highly variable. Because of the highly variable $^{87}Sr/^{86}Sr$ in the G-B river system, it is difficult to arrive at a reliable average $^{87}Sr/^{86}Sr$ value; in the following, we carry out calculations both with our new lower value (0.717) as well as that of Galy *et al.* (*9*) (~0.73). We use the total G-B river water Sr flux of 0.65×10^9 mol/year from Galy *et al.* (*9*).

Using our new groundwater data, we obtain an average dissolved Sr content of 4.5 μmol/liter. We thus obtain an additional subsurface groundwater Sr flux of 0.9×10^{15} μmol/year, which is about 1.4 times the combined G-B riverine Sr flux to the oceans (Table 2). As shown in Table 1, many of the coastal groundwaters have a $^{87}Sr/^{86}Sr$ of about 0.715, whereas inland values are typically somewhat higher than 0.72. Thus, a likely range of $^{87}Sr/^{86}Sr$ ratio in groundwater to the ocean is 0.715 to 0.720. Combining these, we obtain a total flux (river and groundwater) from this system to the oceans for Sr of 1.55×10^9 mol/year, with $^{87}Sr/^{86}Sr$ in the range of ~0.716 to 0.724. These results document the important contributions of groundwater discharge of Sr through the Bengal flood plain as a significant portion of the Himalayan drainage, and this flux must be taken into account in any model for the global exogenic Sr cycle.

In the second part of Table 2, we use published (*1, 4, 7, 9, 19, 22*) as well as our new estimates for the global Sr cycle. The total G-B flux compared to the global continental flux of Sr to the oceans is $J_{GB}/J_{total} = 0.031$, or ~3%. This increased flux results in a new and shorter oceanic residence time for Sr of $\tau_{Sr} = 2$ My. Thus, use of the groundwater estimates in Table 2 suggests that the global continental Sr flux is ~50% higher than that used before.

The global cycle is modeled using the following $^{87}Sr/^{86}Sr$ (= α_{Sr}) isotope mass balance

$$N_{Sr}\left(\frac{d\alpha_{Sr-SW}}{dt}\right) = \sum_i J_i(\alpha_{Sr-i} - \alpha_{Sr-SW}) \quad (1)$$

where J_i is the Sr flux from reservoir i, α_{Sr-i} is the Sr isotopic composition of this flux, SW is seawater, and N_{Sr} is the mass of Sr in the oceans. Estimates of the present values of the $J_i(\alpha_{Sr-i} - \alpha_{Sr-SW})$ terms are given in the last column of Table 2. Note that although the G-B flux is only 3% of the total continental Sr flux to the oceans, it accounts for between 11% of the global isotope balance using the low $^{87}Sr/^{86}Sr$ value (0.7158) and 26% using the high value of $^{87}Sr/^{86}Sr$ (0.7242). Over the past 40 My, seafloor spreading rates were essentially constant (*23*). Thus, the hydrothermal contribution to the Sr cycle was most likely constant over this period of time, and the reason for the global rise in $^{87}Sr/^{86}Sr$ must be either an in-

Table 1. Sr-isotopic compositions and concentrations (C_{Sr}) in Bengal Basin groundwaters and river waters. Where more than one sample was analyzed, averages and ranges are shown. *n* is number of samples measured. Strontium concentrations were measured by inductively coupled plasma mass spectrometry and the $^{87}Sr/^{86}Sr$ by thermal ionization mass spectrometry, both at the University of Rochester. Errors in Sr concentration determinations are usually less than 3% and for individual Sr isotope ratio measurements, normalized to $^{86}Sr/^{88}Sr = 0.1194$, the errors in 2σ of the mean correspond to less than 3 in the fifth decimal place. The NBS 987 Sr standard gave $^{87}Sr/^{86}Sr = 0.710246 \pm 28$ ($n = 8$) during the course of these measurements.

Location	Depth (m)	Average C_{Sr} (μmol/liter)	$^{87}Sr/^{86}Sr$ range	$^{87}Sr/^{86}Sr$ average	*n*
		Groundwaters (coastal)			
Laxmipur	150–244	4.64	0.7133–0.7156	0.71502	3
Barisal	290–335	1.09	0.7145–0.7149	0.71469	2
Burir Char	61	1.11	–	0.71431	1
Baruipur	293	5.06	–	0.72113	1
Barasat	18–207	5.17	0.7215–0.7270	0.72446	8
		Groundwaters (inland)			
Samta	9–100	4.64	0.7240–0.7273	0.72668	4
Madaripur	30	3.01	–	0.72682	1
Faridpur-Rajbari	20–244	4.24	0.7174–0.7240	0.72018	11
Sonargaon	27–91	3.09	0.7124–0.7190	0.71781	4
Meherpur	27–40	4.87	0.7214–0.7251	0.72431	5
Kustia	33–88	3.97	0.7196–0.7254	0.72373	5
Ishurdi	18–36	5.10	0.7107–0.7245	0.72039	6
Nawabganj	9–34	6.11	0.7271–0.7348	0.72916	3
Shibganj	42	5.29	–	0.73094	1
		River waters			
Brahmaputra		0.64	0.7171–0.7172	0.71712	2
Meghna		1.04	–	0.71618	1
Dhaleshwari		0.50	–	0.71952	1
Ganges		0.59	0.7243–0.7249	0.72458	2

Table 2. The Ganges-Brahmaputra river and groundwater Sr isotopic balance and the global marine Sr isotopic mass balance. The total mass of Sr in seawater is 1.25×10^{17} mol.

	Water flux (liter/year)	C_{Sr} (μmol/liter)	J_{Sr} (μmol/year)	$^{87}Sr/^{86}Sr$	$J_i(\alpha_{Sr-i}-\alpha_{Sr-SW})$ (μmol/year)
		Ganges-Brahmaputra			
River water	1.07×10^{15}*	0.61	0.65×10^{15}*	0.7170†	0.51×10^{13}
				0.7300†	1.35×10^{13}
Groundwater	0.2×10^{15}†	4.5†	0.90×10^{15}	0.7150†	0.52×10^{13}
				0.7200†	0.97×10^{13}
Total flux	1.27×10^{15}	1.22	1.55×10^{15}	0.7158	1.02×10^{13}
				0.7242	2.33×10^{13}
		Global			
River water	4.24×10^{16}‖	0.78	3.3×10^{16}‡	0.711‡	5.94×10^{13}
Groundwater	0.238×10^{16}§	6.93§	1.65×10^{16}†	0.711	2.97×10^{13}
Total continental flux	4.478×10^{16}	1.11	4.95×10^{16}	0.711	8.91×10^{13}
Hydrothermal water	1.095×10^{14}	91.3‡	1.0×10^{16}‡	0.7035‡	-5.74×10^{13}
Diagenetic flux	3.29×10^{13}	91.3‡	0.3×10^{16}‡	0.7084‡	-0.24×10^{13}
Seawater	–	91.3	–	0.7092‡	

*Values from Galy *et al.* (*9, 19*). †Values suggested by this work. ‡Values used by Richter *et al.* (*4*) based on Goldstein and Jacobsen (*1*) and Palmer and Edmond (*7*). §See (*22*). ‖Korzun (*24*).

crease in the total continental flux of Sr or a change in its isotopic composition, or both. The contribution of G-B to the global cycle

$$\left(\frac{d\alpha_{Sr-SW}}{dt}\right) = \left(\frac{J_{GB}}{N_{Sr}}\right) \cdot (\alpha_{Sr-GB} - \alpha_{Sr-SW}) \quad (2)$$

is equal to 0.82×10^{-4} My^{-1} for the low estimate of $^{87}Sr/^{86}Sr$ and 1.86×10^{-4} My^{-1} for the high estimate of $^{87}Sr/^{86}Sr$ in Table 2. This rate of change is a factor of ~2.3 to 5.3 higher than the observed average value of $d\alpha_{Sr-SW}/dt \sim 0.35 \times 10^{-4}$ My^{-1} for the past 40 My.

We also note that use of a $^{87}Sr/^{86}Sr$ value of 0.711 for global river and continental flux creates an imbalance in the Sr cycle. To rectify this situation, we need to lower the continental flux isotopic composition to about 0.71049 [similar to the value proposed in (*1*)]. Also, the additional global continental Sr flux from groundwater would cause a rise in $^{87}Sr/^{86}Sr$ of 0.0095 over 40 My if left unbalanced. This is higher by a factor of 7 than the observed rise over the past 40 My.

Thus, we conclude that the groundwater data have an enormous effect on the interpretation of the seawater Sr isotope balance. Although we do not claim that the new values presented in Table 2 should be considered as final, these data urge caution about overinterpreting Sr isotope data from a few local watersheds in this area. For example, trying to use the seawater Sr isotope curve to infer the detailed tectonic uplift history of the Himalayas as well as for estimating effects on global climate change still involves considerable uncertainty. Because of the highly variable nature of $^{87}Sr/^{86}Sr$ in the G-B river system, reliable average values are difficult to estimate.

References and Notes

1. S. J. Goldstein, S. B. Jacobsen, *Chem. Geol. Isotope Geosci. Sect.* **66**, 245 (1987).
2. S. B. Jacobsen, *Earth Planet. Sci. Lett.* **90**, 315 (1988).
3. J. M. Edmond, *Science* **258**, 1594 (1992).
4. F. M. Richter, D. B. Rowley, D. J. DePaolo, *Earth Planet. Sci. Lett.* **109**, 11 (1992).
5. S. B. Jacobsen, A. J. Kaufman, *Chem. Geol.* **161**, 37 (1999).
6. S. Krishnaswami, J. R. Trivedi, M. M. Sarin, R. Ramesh, K. K. Sharma, *Earth Planet. Sci. Lett.* **109**, 243 (1992).
7. M. R. Palmer, J. M. Edmond, *Geochim. Cosmochim. Acta* **56**, 2099 (1992).
8. M. E. Raymo, W. F. Ruddiman, *Nature* **359**, 117 (1992).
9. A. Galy, C. France-Lanord, L. A. Derry, *Geochim. Cosmochim. Acta* **63**, 1905 (1999).
10. M. Sharma, G. J. Wasserburg, A. W. Hofmann, G. J. Chakrapani, *Geochim. Cosmochim. Acta* **63**, 4005 (1999).
11. L. A. Derry, C. France-Lanord, *Earth Planet. Sci. Lett.* **142**, 59 (1996).
12. N. B. W. Harris, *Geology* **23**, 721 (1995).
13. J. D. Blum, C. A. Gazis, A. D. Jacobsen, C. P. Chamberlain, *Geology* **26**, 411 (1998).
14. J. Quade, L. Roe, P. G. DeCelles, T. P. Ojha, *Science* **276**, 1828 (1997).
15. W. S. Moore, *Nature* **380**, 612 (1996).
16. J. Carroll, K. K. Falkner, E. T. Brown, W. S. Moore, *Geochim. Cosmochim. Acta* **57**, 2981 (1993).
17. W. S. Moore, *Earth Planet. Sci. Lett.* **150**, 141 (1997).
18. N. Harris, M. Bickle, H. Chapman, I. Fairchild, J. Bunbury, *Chem. Geol.* **144**, 205 (1998).
19. A. Galy, C. France-Lanord, *Chem. Geol.* **159**, 31 (1999).
20. C. B. Dowling, R. J. Poreda, A. R. Basu, P. K. Aggarwal, *EOS* (Fall Suppl.) **81**, F524 (2000).
21. Tritium-helium ages of 39 groundwater samples were determined and are being reported elsewhere [C. B. Dowling, R. J. Poreda, A. R. Basu, in preparation.] The ^3H-^3He isotopic ages of samples with higher contents of tritium (4 to 7 tritium units) are consistent with their origin during the nuclear test era. Tritiated water is found to a depth of 150 m in some areas, implying highly conductive sediments. The ratio of tritiogenic $^3He^*$ to ^3H gives a subsurface travel time for groundwater containing tritium. This velocity ranges from 3 m/year in the active flow system to <0.5 m/year in the low-flow zone. Overall, the groundwater age data establish an average recharge rate of 0.6 ± 0.2 m/year. In the highly conductive sediments of the Bengal Basin, the monsoon water is relatively quickly recharged and flushed through the sediments over wide areas of this flood plain. The horizontal hydraulic gradient was found to be very low at the sample collection sites (Fig. 1). The recharged water and the groundwater flowing beneath the river bottom (>30 m) do not discharge to the G-B rivers and their tributaries; only the groundwater from the shallow part of the aquifer (<20 m) will discharge to the G-B rivers and contribute to the base flow of the rivers. Thus, the groundwater flux to the oceans is estimated here on the basis of the average groundwater travel time below 30 m.
22. Based on estimates of groundwater influx to the oceans and groundwater salt loading by I. S. Zekster and H. A. Loaiciga [*J. Hydrol.* **144**, 405 (1993)].
23. C. Lithgow-Bertelloni, M. A. Richards, Y. Ricard, R. J. O'Connell, D. C. Engebretson, *Geophys. Res. Lett.* **20**, 375 (1993).
24. V. I. Korzun, *Studies and Reports in Hydrology*, vol. 25 (Unesco, Paris, 1978).

25. We thank the Atomic Energy Center and the Water Development Board of Bangladesh, and the Central Groundwater Board, West Bengal, India for providing field assistance in water sample collection. The International Atomic Energy Agency (Vienna, Austria) sponsored this activity. This research was partially supported by NSF grants helpful. We also thank two anonymous reviewers for their helpful comments.

8 March 2001; accepted 17 July 2001

Genetic Evidence for Two Species of Elephant in Africa

Alfred L. Roca,[1] Nicholas Georgiadis,[2] Jill Pecon-Slattery,[1] Stephen J. O'Brien[1]*

Elephants from the tropical forests of Africa are morphologically distinct from savannah or bush elephants. Dart-biopsy samples from 195 free-ranging African elephants in 21 populations were examined for DNA sequence variation in four nuclear genes (1732 base pairs). Phylogenetic distinctions between African forest elephant and savannah elephant populations corresponded to 58% of the difference in the same genes between elephant genera *Loxodonta* (African) and *Elephas* (Asian). Large genetic distance, multiple genetically fixed nucleotide site differences, morphological and habitat distinctions, and extremely limited hybridization of gene flow between forest and savannah elephants support the recognition and conservation management of two African species: *Loxodonta africana* and *Loxodonta cyclotis*.

Conservation strategies for African elephants have consistently been based on the consensus that all belong to the single species *Loxodonta africana* (*1–3*). Yet relative to African savannah elephants, the elephants in Africa's tropical forests are smaller, with straighter and thinner tusks, rounded ears, and distinct skull morphology (*2–11*). Although forest elephants are sometimes assigned subspecific status and designated *L. a. cyclotis*, their degree of distinctiveness and of hybridization with savannah elephants has been controversial and often ignored (*2–12*). Recently, a comprehensive morphological comparison of metric skull measurement from 295 elephants (*10*, *11*) and a provocative molecular report limited to a single individual (*13*) noted appreciable distinctions between forest and savannah specimens.

Here we report the patterns and extent of sequence divergence for 1732 nucleotides from four nuclear genes (*14*) among 195 African elephants collected across their range in Africa and from seven Asian elephants (*Elephas maximus*). African elephants were sampled, with biopsy darts (*15*, *16*), throughout the continent, including individuals from 21 populations in 11 of 37 African elephant range nations (Fig. 1). Based on morphology (*2–11*) and habitat (*17*, *18*), three populations were categorized as African forest elephants, whereas 15 populations in southern, eastern, and north-central Africa were categorized as savannah elephants (Fig. 1). DNA sequences from four nuclear genes, including short exon segments (used to establish homology to mammalian genes) and longer introns (which would evolve rapidly enough to be phylogenetically informative), were determined for all elephants (*19*). The genes include *BGN* [646 base pairs (bp)], *CHRNA1* (655 bp),

[1]Laboratory of Genomic Diversity, National Cancer Institute, Frederick, MD 21702, USA. [2]Mpala Research Center, Post Office Box 555, Nanyuki, Kenya.

*To whom correspondence should be addressed. E-mail: obrien@ncifcrf.gov